Quantum Mechanical and Molecular Dynamical Simulations on Thorium(IV) Hydrates in Aqueous Solution

Tianxiao Yang,* Satoru Tsushima, and Atsuyuki Suzuki

Department of Quantum Engineering and Systems Science, School of Engineering, The University of Tokyo, Hongo 7-3-1, Bunkyo, Tokyo 113-8656, Japan

Received: June 21, 2001; In Final Form: September 13, 2001

We report the combined quantum mechanical and molecular dynamical simulations on thorium(IV) hydrates in aqueous solution. Hydration of the Th^{4+} ion in aqueous system was first investigated using the B3LYP hybrid density functional theoretical calculations. The results show that the first shell hydration number of Th^{4+} ion in liquid phase is 9 at the bond distance of Th−O_I 2.54(1) Å and Th−H_I 3.22(1) Å. Second, the second shell hydration properties of the Th^{4+} ion in aqueous solution were studied by the molecular dynamical simulation using AMBER force field. The concept of the hydrated ion was used, $[Th(H_2O)_9]^{4+}$ being the cationic entity interacting in solution. The $[Th(H_2O)_9]^{4+}$−water interaction potential was developed by ab intio B3LYP calculations. The partial atomic charge of $[Th(H_2O)_9]^{4+}$ is derived from the ESP method. The MD calculated results show a well-defined second coordination shell and an ill-defined third shell around the $[Th(H_2O)_9]^{4+}$ ion. The strong hydrogen bonding due to the polarization of the first coordination sphere water molecules leads to a mean coordination number of 18.9 water molecules in the second shell at the bond distance of Th−O_{II} 4.75 Å and Th−H_{II} 5.35 Å. The residence time of a water molecule in the second hydration shell is 423.4 ps. Our simulated results indicate that the hydrated ion concept for simulating the Th^{4+} ion in aqueous solution is appropriate.

1. Introduction

Characterization of the hydrated properties of the thorium(IV) ion represents not only an important theme in aqueous chemistry, but also a reference for further studies on tetravalent actinide(IV) aqua ions. Recently, several papers reported the experimental studies on the hydration of thorium(IV) in aqueous solution.[1−5] Johansson et al.[1] have studied the coordination around the thorium(IV) ion in aqueous perchlorate, chloride, and nitrate solutions using large angle X-ray scattering measurements. They reported that the coordination number of the Th^{4+} ion in aqueous solution depends on the counterions. In the presence of the noncomplex-forming perchlorate ions, the coordination number is eight and independent of concentration. The coordination number increases in the presence of the weakly complex-forming chloride ions. In the nitrate solutions, the coordination number increases to about ten. They have found that about 20 water molecules are present in the second coordination sphere in dilute perchlorate solutions. Moll et al.[2] and Sandström et al.[3] have studied the structure and the hydration of aqueous thorium(IV) ion using EXAFS (Extended X-ray Absorption Fine Structure) measurements. They reported that the first shell coordination number is in the range 9−11 at the bond distance of 2.45 Å. Farkas and co-workers[4] have studied the water exchange of the thorium(IV) aqua ion using ^{17}O NMR measurements. They suggested a dissociatively activated interchange mechanism for the Th(IV) ion, and determined a minimum value for the rate constant at room temperature $k_{exTh^{4+}} > 5 \times 10^7\ s^{-1}$. Hovey[5] made a thermodynamic study of the hydration of the Th^{4+} aqua ion. Recently, other groups[6,7] have studied the structures and the properties of the thorium tetrahalides using the density functional theory. But to our knowledge, there are no theoretical simulation results on the hydrated properties of the Th^{4+} ion in aqueous solution. The experimental data from EXAFS or NMR kinetic measurements for the second coordination sphere are still lacking for the Th(IV) ion. The knowledge on the water exchange rates and the kinetic behaviors of the second sphere water molecules is even scarce.

Computer simulations, in particular the quantum mechanical (QM) and the molecular dynamical (MD) simulations, have provided theoretical approaches to elucidate the structure and the dynamics of molecules during the last two decades. However, the success of the molecular dynamical results strongly depends on the interaction potentials used to describe the forces acting among the components of the model system.[8−9] One of the most usual assumptions to describe the particle interactions is that of the pairwise additivity.[9] However, in the case of highly charged cations immersed in polar solvents such as water, such a premise fails mainly due to the neglect of the nonadditive behavior of the classical electric polarization.[10] A strategy that overcomes to a great extent this difficulty is the use of the hydrated ion, $[M(H_2O)_n]^{m+}$, as the representative entity in solution, instead of the bare ion.[9] In this case, the bare ion−water interaction potential is replaced by the hydrated ion−water one. The Pappalardo et al.[11] have successfully used this method to develop ab initio hydrated ion−water potentials for small and highly charged cations including Be^{2+}, Mg^{2+}, Al^{3+}, Cr^{3+}, and Zn^{2+}. The validity of this approach has also been demonstrated by Bleuzen et al.[12]

In the present work, we introduced the hydrated ion concept for the highly charged Th^{4+} ion to simulate its properties in solution. We first calculated the hydrated properties of the primary hydration sphere of the Th(IV) ion using ab initio B3LYP hydrid density functional theoretical calculations. With

* Corresponding author. Fax: +81-3-3818-3455. E-mail: txyang@lyman.q.t.u-tokyo.ac.jp.

10.1021/jp012387d CCC: $20.00
Published on Web 10/20/2001

respect to the quantum mechanical calculation, Th(IV) is easier for theoretical treatment among the actinide ions because of its d^0f^0 electronic configuration and its closed-shell ground state. We determined its first hydration shell coordination number to be 9. For the following molecular dynamical calculations, $[Th(H_2O)_9]^{4+}$ is considered as an entity present in aqueous solution. It is particularly appropriate since its first-shell water exchange rate constant is small enough to consider the hydrate as a stable polynuclear tetravalent cation.

2. Quantum Mechanical Calculation of $[Th(H_2O)_n]^{4+}$ in Aqueous Solution

2.1. Computational Method. To perform the molecular dynamical (MD) simulations on the second coordination sphere, we first performed the quantum mechanical calculations on the Th^{4+} ion to obtain its geometry and the first coordination sphere information.

The calculations were run with Gaussian 98 package of programs.[13] The B3LYP hybrid density functional method (Becke's three parameter hybrid functional using the LYP correlation functional[14,15]) was used, since this method is known to reproduce accurate geometries and thermochemistries for the transition metals and uranium complexes.[16−17] Spin−orbit effects were not considered here, since they are less important for the closed shell system being considered here.

The calculations employed the relativistic large core effective core potential (RECP) developed by Küchle et al.[18] and the corresponding basis set for thorium. The 6-31G* all electron basis sets were used for oxygen and hydrogen.[19]

We calculated the Gibbs free energy of the molecules in the aqueous phase, where the solvation energy and the entropy were included. Solvation energies were calculated using polarized continuum model (PCM) method of Tomasi and co-workers[20] (SCRF═PCM in Gaussian 98). Scaling factor 1.2 was used for the definition of the solvent accessible surface of all elements except hydrogen. So the radius of each atomic sphere was determined by multiplying the van der Waals radius by the scaling factor. In our previous work,[21] we have a specific explanation of the calculations of the solvation energy, the entropy and the binding energy in aqueous phase.

2.2. Calculated Results and Discussion. Several papers have studied the hydration numbers of actinide elements theoretically. Tsushima et al.[22] and Spencer et al.[23] have reported the hydration numbers of pentavalent and hexavalent uranyl, neptunyl, and plutonyl ions through "gas phase" calculations. Blaudeau et al.[24] have published a paper on the structures of $Pu(H_2O)_n^{3+}$ clusters. Recently, Antonio et al.[25] have studied the neptunium redox speciation. All these works have discussed the stability of the hydrated complexes from the electronic energy in gas phase under Born−Oppenheimer approximation, which is the energy at 0 K and 0 atm. We have recently reported the hydration properties of $UO_2(H_2O)_n^{2+}$ in aqueous solution.[21] We have discussed that the inclusion of the solvation energy and the concentration correction into the gas-phase Gibbs free energy is very crucial in studying the hydration properties.

In the present work, sixteen different thorium(IV) hydrated clusters $[Th(H_2O)_n^{4+}](n = 6,8,9,10,12)$ were investigated (Table 1). The initial geometric structures of $[Th(H_2O)_n(H_2O)_h]^{4+}$ (n = first shell, h = second shell) clusters are created using the same approach as the previous work.[21] The coordination geometries were optimized in vacuo. The inclusion of the bulk solvent effects by PCM on aquo-ions of heavy metals and a thorough discussion of computational aspects have been given by Cosentino et al.[26] Their studies have shown that though the surrounding effects should be included in the geometry optimization to obtain molecular structures in better agreement with solid state and solution experimental structures, the energetics of these systems can be appropriately calculated in vacuo optimized structures because the term due to the geometry relaxation in solution is not significant. The calculated binding energies of the clusters of $[Th(H_2O)_n(H_2O)_h]^{4+}$ are summarized in Table 1. The gas-phase binding energy is derived from the Gibbs free energy difference between the product and the sum of its molecular components. The aqueous phase binding energy includes the PCM (Polarized Continuum Model) solvation energy and the entropic correction[21,27] into the Gibbs free energy. The correlation effects in the gas-phase complexation reaction are relevant in determining correct hydration free energies, while they do not play any significant role in the aqueous ion solvation. Our results are in good accordance with that of Cosentino et al., though the method of calculating the correlation effects is different.

TABLE 1: Calculated Binding Energy (in kcal/mol) of the $Th(H_2O)_n(H_2O)_h^{4+}$ Clusters

total water numbers ($n + h$)	clusters	gas phase	aqueous phase
6	$Th^{4+}\cdot 6H_2O(T_h)$	−724.12	−121.09
8	$Th^{4+}\cdot 6H_2O\cdot 2H_2O$	−742.38	−160.32
	$Th^{4+}\cdot 8H_2O(D_{2d})$	−747.26	−163.11
9	$Th^{4+}\cdot 9H_2O(C_{4v})$	−785.23	−148.73
	$Th^{4+}\cdot 9H_2O(D_{3h})$	−777.02	−144.65
	$Th^{4+}\cdot 8H_2O\cdot H_2O(C_{2v})$	−789.47	−136.32
10	$Th^{4+}\cdot 6H_2O\cdot 4H_2O(T_h)$	−782.44	−134.51
	$Th^{4+}\cdot 8H_2O\cdot 2H_2O(D_{2d})$	−820.09	−143.44
	$Th^{4+}\cdot 9H_2O\cdot H_2O(C_{4v})$	−815.33	−157.92
	$Th^{4+}\cdot 10H_2O(D_{4d})$	−804.71	−157.22
	$Th^{4+}\cdot 10H_2O(D_{5d})$	−756.07	−119.27
12	$Th^{4+}\cdot 8H_2O\cdot 4H_2O$	−894.31	−165.88
	$Th^{4+}\cdot 9H_2O\cdot 3H_2O$	−888.09	−173.57
	$Th^{4+}\cdot 10H_2O\cdot 2H_2O(D_{4d})$	−872.56	−173.28
	$Th^{4+}\cdot 12H_2O(D_{2d})$	−801.53	−123.36
	$Th^{4+}\cdot 12H_2O(D_{2h})$	−820.09	−122.94

Based on the binding energies of the different hydration numbers and symmetries, it is possible to acknowledge the most stable structure. From Table 1, it is very clear that for the $[Th(H_2O)_n^{4+}]$ cluster, when the total number of hydration water molecules is 9, $Th(H_2O)_9^{4+}$ with C_{4v} symmetry has the lowest binding energy. When the total hydration water molecules is 10, $Th^{4+}\cdot 9H_2O\cdot H_2O(C_{4v})$ has the lowest binding energy, while when the total hydration water molecules is 12, $Th^{4+}\cdot 9H_2O\cdot 3H_2O$ has the lowest binding energy. However, the binding energy differences between $Th^{4+}\cdot 9H_2O\cdot H_2O(C_{4v})$ and $Th^{4+}\cdot 10H_2O(D_{4d})$, $Th^{4+}\cdot 9H_2O\cdot 3H_2O(C_{4v})$ and $Th^{4+}\cdot 10H_2O\cdot 2H_2O(D_{4d})$ are not significant. We are led to conclude that $Th(H_2O)_9^{4+}$ with C_{4v} symmetry can form the most stable complex, the coordination number of water molecules around the Th(IV) ion in the first shell is 9.

For $Th(H_2O)_9^{4+}$, three possible structures were investigated, a D_{3h} tricapped-trigonal-prismatic arrangement of the oxygen atoms (Figure 1a), a C_{4v} capped-square-antiprism arrangement of the oxygen atoms (Figure 1b), and a C_{2v} "8+1" structure in which one water molecule was moved outside of its first solvation shell of eight water molecules (Figure 1c). The C_{4v} structure is more stable than the D_{3h} structure for the $Th(H_2O)_9^{4+}$ complex. Zhang et al.[28] studied the coordination polyhedron of the thorium(IV) malonato compounds. They have found that, in the $(C_2H_{10}N_2)_2[Th(C_3H_2O_4)_4(H_2O)]$ compound, there are nine oxygens which are directly coordinated to the central Th atom,

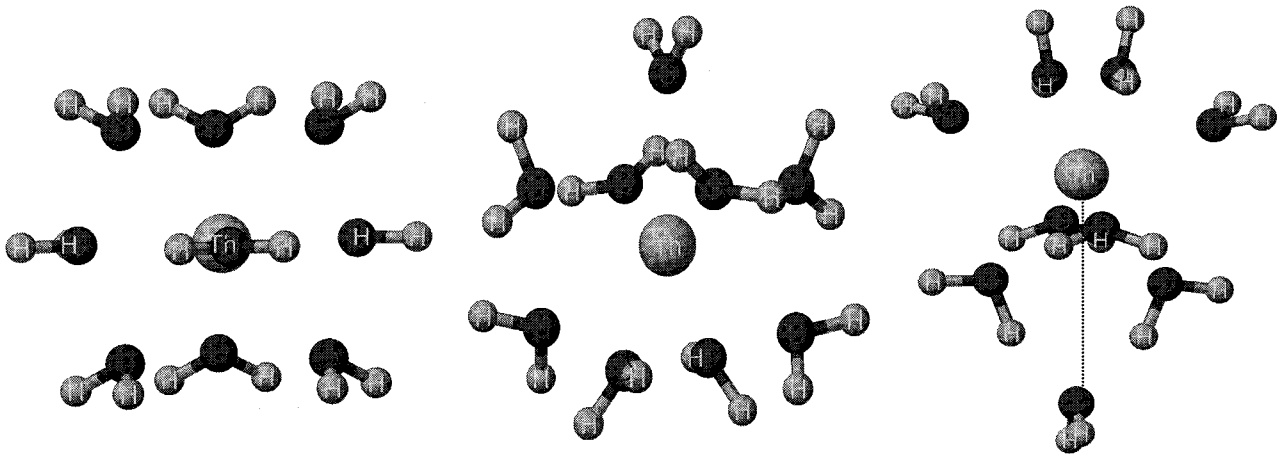

Figure 1. The optimized structures of the $[Th(H_2O)_9]^{4+}$ with different geometries, D_{3h} (upper left), C_{4v} (upper right), and C_{2v}"8 + 1"(below).

and they show a capped square antiprismatic geometry having the C_{4v} symmetry. Kowall et al.[29] reported that the D_{3h} symmetry is the most stable structure for the $[Ln(H_2O)_9]^{3+}$ complexes. The difference in the symmetry between $Th(H_2O)_9^{4+}$ and $Ln(H_2O)_9^{3+}$ may be attributed to the characters of the 6*d* and 5*f* orbitals. The Mulliken population of the 6*d* and 5*f* orbitals of Th is quite similar in the C_{4v} and D_{3h} structures. Both structures have 1.0 and 0.8 *e* for the 6*d* and 5*f* population, respectively. The major difference is the transfer of 0.08 *e* from the 5$f\varphi$ to 5$f\sigma$ and 5$f\pi$ orbitals, and the transfer of 0.04 *e* from the 6$d\delta$ to 6$d\sigma$ orbitals. The Th 6*d* and 5*f* orbitals are much more degenerate in the D_{3h} structure than in the C_{4v} structure because the former has the higher symmetry. In essence, the C_{4v} structure leads to greater overlapping between the Th 6*d*, 5*f* orbitals and the O 2*p* orbitals. Additionally, a vibrational frequency calculation of the C_{4v} structure resulted in all positive frequencies, indicating that this structure truly is a minimum. The geometry and the partial atomic charge of $Th(H_2O)_9^{4+}$ with the C_{4v} symmetry are used for the following molecular dynamical simulations. $Th(H_2O)_9^{4+}$ shows an asymmetric distribution of the thorium−oxygen bond distances in the range of 2.54−2.55 Å, and the thorium−hydrogen distances in the range of 3.22−3.23 Å. Sandström et al.[3] also reported the asymmetric distribution of the Th−O bond distance in the order of ±0.01 Å on the basis of EXAFS measurements.

The atomic charges of the $Th(H_2O)_9^{4+}$ ion deriving from different techniques are tabulated in Table 2. It is clear that the Mulliken population analysis gives too underestimated positive charge on the metal. It was already discussed by other groups[12,30−31] that the Mulliken charges do not seem to model properly the charge distribution. The charge distributions of the $Th(H_2O)_9^{4+}$ ion were calculated using the ESP (electrostatic potential) method[32] and the CHELPG procedure.[33] The fitting requires the atomic radii for the construction of the surface where the electrostatic potential is calculated. But as there is no default radius for thorium in the Gaussian program, we tried different radius values from 1.2 to 2.5 Å (Table 2). For the ESP method, the partial atomic charges keep constant as the thorium radius changes from 1.2 to 1.8 Å, and a small variation of 0.16 *e* for thorium as its radius increases up to 2.2 Å. For the same atomic radius, the CHELPG method generally gives larger metal atomic charge than the ESP. We finally assigned 3.02 *e* (derived from the ESP method) charge to thorium, −1.02 to −1.04 *e* to oxygen atoms, and 0.56−0.57 *e* to hydrogen atoms, respectively.

TABLE 2: Atomic Charges Calculated for the $[Th(H_2O)_9]^{4+}$ System Using Different Techniques[a]

Th radius/Å	method	q_{Th}	q_O	q_H
	Mulliken	1.572	−0.801 to −0.803	0.534−0.538
1.2	ESP	3.028	−1.025 to −1.045	0.567−0.576
	CHELPG	3.549	−1.120 to −1.171	0.588−0.611
1.5	ESP	3.028	−1.025 to −1.046	0.567−0.575
	CHELPG	3.247	−1.056 to −1.085	0.572−0.586
1.8	ESP	3.028	−1.025 to −1.046	0.567−0.576
	CHELPG	3.126	−1.027 to −1.054	0.565−0.577
2.0	ESP	2.905	−1.003 to −1.020	0.564−0.571
	CHELPG	3.081	−1.016 to −1.043	0.562−0.575
2.2	ESP	2.865	−0.997 to −1.013	0.563−0.569
	CHELPG	3.027	−1.006 to −1.032	0.560−0.571
2.4	ESP	2.801	−0.9897 to −1.007	0.561−0.568
	CHELPG	2.972	−0.996 to −1.022	0.557−0.570
2.5	ESP	2.769	−0.985 to −0.999	0.563−0.566
	CHELPG	2.933	−0.991 to −1.012	0.557−0.566

[a] The partial atomic charge of $Th(H_2O)_9^{4+}$ has an asymmetric distribution because of its asymmetric distribution of the $Th-O_I$ bond distance, i.e., 9 water oxygen atoms and 18 hydrogen atoms have different charge distribution.

3. Molecular Dynamical Calculation of $[Th(H_2O)_9^{4+}]$ in Aqueous Solution

3.1. Computational Method. The calculations were performed with the program package AMBER6.0.[34] As was discussed in the Introduction section, the use of the hydrated ion concept can overcome to some extent the difficulties such as the electric polarization due to the exchange contributions and the charge transfer.[9] Therefore, the hydrated ion concept was used for Th(IV), $[Th(H_2O)_9^{4+}]$ being the cationic entity interacting in solution. All interaction potentials in our simulations were of pair potential type and consisted of a Coulomb part and a Lennard-Jones part (LJ) (eq 1)

$$E(r) = q_i q_j / r - 2\epsilon(R^*/r)^6 + \epsilon(R^*/r)^{12} \qquad (1)$$

where R^* and ϵ are the Lennard-Jones parameters. R^* is the van der Waals radius, ϵ is the potential well depth of the minimum energy point. The simulated model is one $[Th(H_2O)_9^{4+}]$ complex immersed in a periodic box of 569 water molecules together with 4 Cl^- counterions. The bulk and the second sphere water molecules were described using the rigid TIP3P model.[35−36] We abstained from using a flexible water model, which would demand a considerably shorter integration step, but would not

TABLE 3: MD Simulation Conditions and Parameters for $[Th(H_2O)_9]^{4+}$

number of $[Th(H_2O)_9]^{4+}$ complexes	1
number of TIP3P water molecules	569
box size(Å × Å × Å)	30 × 30 × 30
cutoff distance (Å)	15
thorium concentration (M)	0.0615
time step (fs)	0.2
simulation time (ps)	1000
number of stored configurations	20000
temperature (K)	298
pressure (atm)	1
$q_{Th}(e)$	3.02
$q_{O_I}(e)$	−1.02 to −1.04
$q_{H_I}(e)$	0.56−0.57

substantially improve long-time equilibrium properties of liquid water.[36−37] For the geometry and the atomic charges of $[Th(H_2O)_9{}^{4+}]$, we used the results of the previous quantum mechanical calculations (Figure 1 and Table 2). The oxygen and hydrogen atoms were kept fixed (using AMBER6.0 ibelly method[38]) during the MD simulations. Due to the strong interaction of the Th^{4+} ion with the nine first shell oxygen atoms, we could not use the Lennard-Jones parameters of the TIP3P model to describe the interaction between the water molecules of the first shell and the water molecules of the rest.[12] We put LJ parameters of Th^{4+} and the hydrogens (R_{Th}*,R_{H_I}*, ϵ_{Th}, ϵ_{H_I}) to zero. We changed the first shell oxygen Lennard-Jones parameters (R_{O_I}* in the range of 1.0−3.0 Å and ϵ_{O_I} in the range of 0.05−1.20 kcal/mol) to carry out the MD simulations for 200 ps. Finally we found that the first shell oxygen with LJ parameters R_{O_I}* = 2.0 Å and ϵ_{O_I} = 0.08 kcal/mol can best reproduce the experimental bond distance of Th−O_{II}, O_I−O_{II} and the second shell coordination number. Therefore, R_{O_I}* = 2.0 Å and ϵ_{O_I} = 0.08 kcal/mol were used to continue the following MD calculations. The systems were first energy minimized for 1000 steps and equilibrated to the final temperature 298 K at constant volume for 200 ps. The final MD simulation time is 1000 ps. The simulation conditions are listed in Table 3. Half of the box size 15 Å was used as the cutoff distance for nonbonded interactions.

3.2. Calculated Results and Discussion. *3.2.1. Structural Results of the Second Hydration Shell.* According to previous experimental data,[1] in dilute perchlorate solutions a distinct second coordination sphere is present containing about 20 water molecules at the bond distance Th−O_{II} 4.6 Å. Gusev estimated the hydration number of the Th(IV) ion from the dependence of conductance on concentration in $NaClO_4$−$HClO_4$ solutions, and found the second hydration number to be 20.[39] Actually these are the only experimental reports on the second hydration properties of Th^{4+} in aqueous solution because it is very difficult for EXAFS and X-ray scattering measurements to resolve the second hydration shell.

The calculated thorium−oxygen and thorium−hydrogen radial distribution functions $g(r)$ are shown in Figure 2. The peak at 4.75 Å for the oxygen and the peak at 5.35 Å for the hydrogen correspond to the second coordination sphere, which are well-defined. The broad peak at 7.05 Å for oxygen (7.55 Å for hydrogen) corresponds to the third sphere, which is ill-defined. Integration of the oxygen $g(r)$ between 3.50 Å and the first minimum 5.35 Å shows that the mean number of water molecules in the second coordination sphere of Th^{4+} is 18.9. During the MD simulation period of 1000 ps, one of the four Cl^- anions sometimes enters the second coordination shell, but it does not affect the water molecules situating in the second coordination shell. The mean Th−Cl distance of the other three Cl^- anions is 7.5 Å. It shows that these anions locate outside

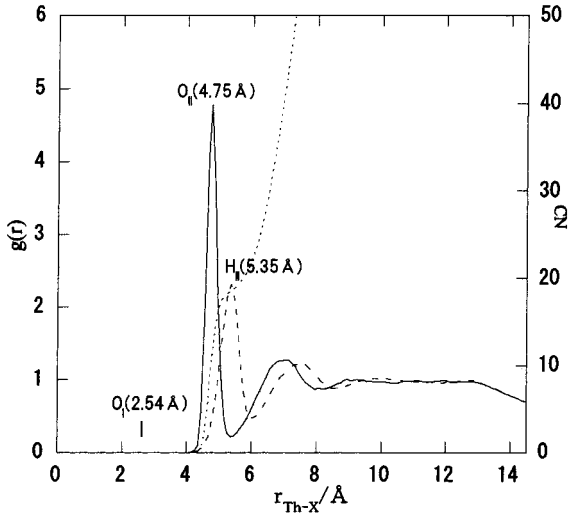

Figure 2. Radial pair distribution function $g(r)$ and running coordination number CN.

TABLE 4: Summary of the Structural and Dynamic Results after 1000 ps MD Simulation of $[Th(H_2O)_9]^{4+}$ in a Periodic Box

system	$[Th(H_2O)_9]^{4+} + 569H_2O + 4Cl^-$
box size (Å)	30 × 30 × 30
$r_{Th-O_{II}}$(Å)	4.75
$r_{Th-H_{II}}$(Å)	5.35
$r_{O_I-O_{II}}$(Å)	2.75
$r_{H_I-O_{II}}$(Å)	1.75
water CN	18.9
$g(r)_{min}$(Å)	5.35
τ_{res}(ps)	423.4
T (K)	298
density (g/cm^3)	1.02

of the third hydration shell. The summarized MD calculated results are shown in Table 4.

3.2.2. Water Exchange between the Second Hydration Shell and the Bulk. The coordination number is defined solely in terms of static quantities.[40] A microscopic structure of the solvation phenomenon and the dynamics of the hydration shell water molecules can be obtained through the observation of the water exchange process. Farkas et al.[4] recently have reported the experimental results on the kinetic parameters for the water exchange of M^{4+} ion. They suggested a dissociatively activated interchange mechanism for Th(IV) between the first hydration shell and the second hydration shell. They determined a minimum value for the rate constant at room temperature and found that the rate constant of the water exchange in the aqueous Th^{4+} ion is at least 1 order of magnitude larger than that for the aqueous U^{4+} ion. Currently no experimental or theoretical data on the water exchange between the second hydration shell and the bulk are reported.

The residence time of a water molecule in the hydration shell gives deeper specific insight into the ionic hydration and the ionic mobility.[40] We calculated the mean lifetime of a water molecule in the second coordination sphere, τ_{res}, using the method described in ref 29 and ref 36. The residence time is based on the definition of $n_{ion}(t)$, which measures the number of molecules that are in a given region around the ion after a period of time t. From this definition, $n_{ion}(0)$ is the number of water molecules in a given region. If this region is the first hydration shell, $n_{ion}(0)$ represents the dynamical hydration number of the first shell. Excluding an initial period for which the function decay rapidly, $n_{ion}(t)$ adopts an exponential form, i.e., $n_{ion}(t) \sim e^{-t/\tau}$, where τ represents a correlation or relaxation

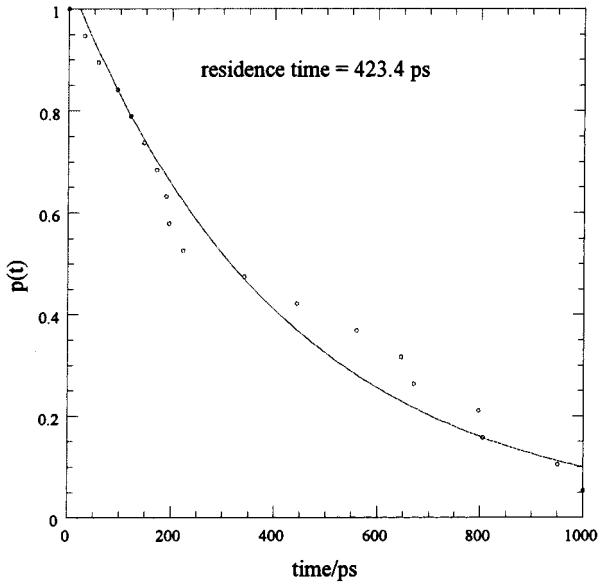

Figure 3. Residence probability $p(t)$ that a water molecule still belongs to the second hydration shell after a correlation time t calculated from MD simulation. Exponential fits are shown as solid line.

time characteristic of the persistence of water molecules in a given region around the ion. This quantity of τ is defined as the residence time of water molecules in that region. The mathematical definition is proposed by Impey et al.[40]

$$n_{ion}(t) = \frac{1}{N_t}\sum_{n=1}^{N_t}\sum_{j} P_j(t_n,t;t^*) \qquad (2)$$

$P_j(t_n,t;t^*)$ is a function that can take only a value of 1 if water molecule j lies within the region considered at both time steps t_n and $t + t_n$ not leaving the region for a period longer than t^*, otherwise $P_j(t_n,t;t^*)$ takes a value of 0. In our calculation, we take t^* the value 2 ps. We calculated the residence probability $p(t)$ of a water molecule at a distance of $r_{Th-O_{II}} \leq 5.35$ Å. 5.35 Å corresponds to the minimum of $g(r)$ after the peak attributed to the second shell oxygens (Figure 2). The residence time τ_{res} obtained by fitting an exponential to $p(t)$ by the least-squares method is 423.4 ps (Figure 3). This residence time corresponds to 45 water exchanges observed in 1000 ps if we account for about 18.9 water molecules in the second sphere.

Basically, all water exchange events should be resolvable into pairs of mutually exchanging water molecules. According to the time difference between a water molecule entering into the second hydration shell and a water molecule leaving from the second hydration shell, the water exchange process is classified as associative, dissociative, or interchange mechanism. Figure 4 characterizes the thorium−oxygen distance for a 10 ps interval. The water exchanges between the second hydration shell and the bulk are observed. It is shown that the crossing point of the trajectories of the incoming and of the leaving water lies in the distance of the third hydration shell water, a dissociative (D) interchange activation mode for the water exchange reaction between the second hydration shell and the third hydration shell is suggested.

By analyzing the trajectories of all the TIP3P water molecules and calculating their mean square displacement, we yielded the diffusion coefficient of water molecules as 2.8×10^{-9} m^2 s^{-1}. Using eq 3

$$\Delta r^2(t) = 6Dt \qquad (3)$$

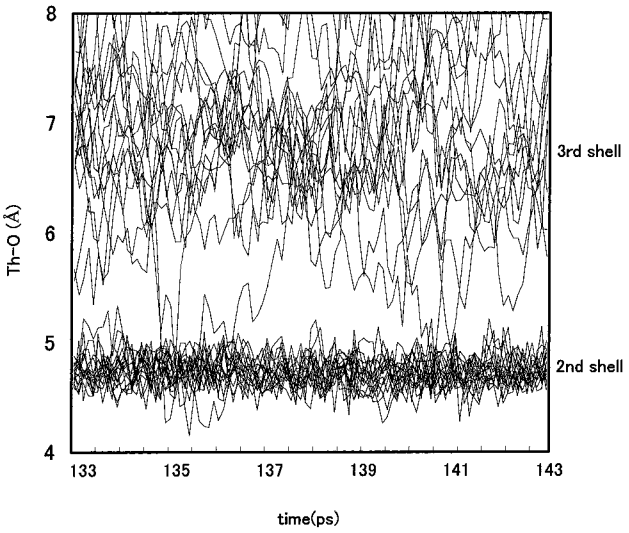

Figure 4. Thorium−oxygen distance for a 10 ps interval showing the water exchange between the second hydration shell and the bulk.

where $\Delta r^2(t)$ is the mean-square displacement, we calculated a time of 2.9 ps for a water molecule to travel the mean distance 2.3 Å between the second and the third hydration coordination shell. This is in fair agreement with what we can see from Figure 4.

3.2.3 Discussion. From ref 4, it can be estimated that the residence time of a water molecule in the first hydration shell is $\tau_{res} = 1/k_{ex} \leq 2 \times 10^4$ ps. Unfortunately, on the experimental side, the kinetic exchange data for the second hydration shell of Th(IV) ion is not available. But a comparison with the trivalent lanthanide complex $[Ln(H_2O)_n]^{3+}$ is instructive. For Nd, Sm, and Yb, the residence time of a water molecule in the first shell is 1577, 170, and 410 ps, respectively, the residence time of a water molecule in the second hydration shell is 13, 12, and 18 ps, respectively.[29] The residence time τ_{res}(second shell) for the Th^{4+} ion is more than 1 order of magnitude higher than that of the Ln^{3+} ions. For the Th(IV) aqua ion, because of its higher positive charge value, it is favorable to form stronger interaction between the Th(IV) ion and water molecules and then form the tight-bonded first hydration shell. Accordingly, the residence time of a water molecule in the first hydration shell is more than 1 order of magnitude higher than that of the Ln^{3+} ions. The fact that the $[Th(H_2O)_9^{4+}]$ unit is interacting with a second hydration shell of about 18.9 water molecules suggests that each water molecule of the first shell binds two water molecules in the second shell, which demonstrates stronger hydrogen bonding between the first hydration water molecules and the second hydration water molecules than the Ln^{3+} ions do. It is not surprising that for the Th^{4+} ion, the residence time of a water molecule in the second shell is over one order higher than that of the trivalent lanthanide complexes. The fact that the lifetime of a water molecule in the second shell of the Th^{4+} ion is 423.4 ps confirms the existence of a well-defined second coordination shell.

The mean distance between the first hydration shell water hydrogen H_I and the second hydration shell water oxygen O_{II} is 1.75 Å (Table 4), which is shorter than the mean hydrogen bond distance found in pure water 1.8−1.9 Å.[12,41−42] This hydrogen bond distance suggests a strong hydrogen-bonding between the first hydration shell and the second shell. This also provides good explanations to the well-defined second hydration shell. The third shell water molecules result in a broad peak in the thorium−oxygen radial distribution function at about 7.05 Å. The hydrogen bond length between the second and the third

coordination shell $H_{II}-O_{III}$ 1.90 Å is within the range of hydrogen bond in pure water. Unfortunately, currently no comparative experimental data is available.

On the whole, our simulation results suggest that our initial structure $[Th(H_2O)_9^{4+}]$ (with C_{4V} geometry), the partial atomic charge distribution and the original interaction potential are reasonable.

For our present MD simulation model, the effect of the polarization of the water molecules was not considered, which probably causes some discrepancy to the actual solvation system. The effect of the nonuniform polarization of the water molecules surrounding the ions has been studied by many authors.[43] To better simulate the actual solvation system, a model including the polarization effect is planned.

Hydrated ion concept assumed that the hydrate was rigid along the simulation.[44] For our simulation model, we fixed the oxygen and hydrogen positions of $[Th(H_2O)_9^{4+}]$. We suppose if we rotate the hydrogens of $[Th(H_2O)_9^{4+}]$, or keep the geometry of $[Th(H_2O)_9^{4+}]$ instead of keeping the solute molecule restraint during the MD calculations, we might expect more results, such as the diffusion coefficient of $[Th(H_2O)_9^{4+}]$ hydrated ion, etc. This is our next step work. In our future work, we will discuss the hydrated properties of the Th^{4+} ion in different counterion systems such as perchlorate, nitrate, and fluoride, the concentration effect will also be included.

4. Conclusions

From our quantum mechanical calculations, we have found that the most stable structure of the hydrated Th^{4+} ion in aqueous solution is $[Th(H_2O)_9^{4+}]$ (with the C_{4v} geometry) and its primary hydration coordination number is 9 at the bond distance of $Th-O_I$ 2.54−2.55 Å. From our combined quantum mechanical and molecular dynamical simulations, we have found a structurally and kinetically well-defined second hydration coordination shell around the Th^{4+} ion in aqueous solution at the bond distance of $Th-O_{II}$ 4.75 Å. The well-defined second hydration coordination shell is formed because of the strong hydrogen bond due to the polarization of the first hydration shell water molecules. The coordination number of water molecules in the second shell is 18.9. The residence time of a water molecule in the second hydration shell is 423.4 ps. The structural and dynamical properties obtained for the Th^{4+} aqueous solutions using the molecular dynamical calculations have a good agreement with experiments. It shows that the hydrated ion concept represents a proper approach to calculate the hydration of Th^{4+} ion in aqueous solution and furthermore the molecular dynamical properties of highly charged atoms such as the actinides.

Acknowledgment. This work was carried out in collaboration with Institut für Radiochemie, Forschungszentrum Rossendorf, Germany. The generous allocation of time on SGI Origin 2000 supercomputer of Technische Universität Dresden is gratefully acknowledged. We thank Dr. Masaru Hirata, Japan Atomic Energy Research Institute, for his advice on various occasions.

References and Notes

(1) Johansson, G.; Magini, M.; Ohtaki, H. *J. Solution Chem.* **1991**, *20*, 775.

(2) Moll, H.; Denecke, M. A.; Jalilehvand, F.; Sandström, M.; Grenthe, I. *Inorg. Chem.* **1999**, *38*, 1795.

(3) Sandström, M.; Persson, I.; Jalilehvand, F.; Lindquist-Reis, P.; Spångberg, D.; Hermansson, K. *J. Synchrotron Radiat.* **2001**, *8*, 657.

(4) Farkas, I.; Grenthe, I.; Bányai, I. *J. Phys. Chem. A* **2000**, *104*, 1201.

(5) Hovey, J. K. *J. Phys. Chem. B* **1997**, *101*, 4321.

(6) Adamo, C.; Barnone, V. *J. Comput. Chem.* **2000**, *21*, 1153.

(7) Gagliardi, L.; Skylaris, C. K.; Willetts, A.; Dyke, J. M.; Barone, V. *Phys. Chem. Chem. Phys.* **2000**, *2*, 3111.

(8) Stone, A. J. *The Theory of Intermolecular Forces;* Clarndon: Oxford, 1996.

(9) Martínez, J. M.; Hernández-Cobos, J.; Saint-Martin, H.; Pappalardo, R. R.; Ortega-Blake, I.; Sánchez Marcos, E. *J. Chem. Phys.* **2000**, *112*, 2339.

(10) Elrod, M. J.; Saykally, R. J. *Chem. Rev.* **1994**, *94*, 1975.

(11) (a) Pappalardo, R. R.; Sánchez Marcos, E. *J. Phys. Chem.* **1993**, *97*, 4500. (b) Pappalardo, R. R.; Martínez, J. M.; Sánchez Marcos, E. *J. Phys. Chem.* **1996**, *100*, 11748. (c) Sánchez Marcos, E.; Martínez, J. M.; Pappalardo, R. R.; *J. Chem. Phys.* **1996**, *105*, 5968. (d) Martínez, J. M.; Pappalardo, R. R.; Sánchez Marcos, E. *J. Chem. Phys.* **1998**, *109*, 1445. (e) Martínez, J. M.; Pappalardo, R. R.; Sánchez Marcos, E. *J. Phys. Chem. B* **1998**, *102*, 3272. (f) Martínez, J. M.; Pappalardo, R. R.; Sánchez Marcos, E.; *J. Am. Chem. Soc.* **1999,** *121*, 3175. (g) Martínez, J. M.; Pappalardo, R. R.; Sánchez Marcos, E. *J. Chem. Phys.* **1999**, *110*, 1669.

(12) Bleuzen, A.; Foglia, F.; Furet, E.; Helm, L.; Merbach, A. E.; Weber, J. *J. Am. Chem. Soc.* **1996**, *118*, 12777.

(13) Frisch, M. J.; Trucks, G. W.; Schlegel, H. B.; Scuseria, G. E.; Robb, M. A.; Cheeseman, J. R.; Zakrzewski, V. G.; Montgomery, J. A.; Stratmann, R. E.; Burant, J. C.; Dapprich, S.; Millam, J. M.; Daniels, A. D.; Kudin, K. N.; Strain, M. C.; Farkas, O.; Tomasi, J.; Barone, V.; Cossi, M.; Cammi, R.; Mennucci, B.; Pomelli, C.; Adamo, C.; Clifford, S.; Ochterski, J.; Petersson, G. A.; Ayala, P. Y.; Cui, Q.; Morokuma, K.; Malick, D. K.; Rabuck, A. D.; Raghavachari, K.; Foresman, J. B.; Cioslowski, J.; Ortiz, J. V.; Stefanov, B. B.; Liu, G.; Liashenko, A.; Piskorz, P.; Komaromi, I.; Gomperts, R.; Martin, R. L.; Fox, D. J.; Keith, T.; Al-Laham, M. A.; Peng, C. Y.; Nanayakkara, A.; Gonzalez, C.; Challacombe, M.; Gill, P. M. W.; Johnson, B. G.; Chen, W.; Wong, M. W.; Andres, J. L.; Head-Gordon, M.; Replogle, E. S.; Pople, J. A. *Gaussian 98, Revision A.6.1*; Gaussian, Inc.: Pittsburgh, PA, 1998.

(14) Becke, A. D. *J. Chem. Phys.* **1993**, *98*, 5648.

(15) Lee, C. T.; Yang, W. T.; Parr, R. G. *Phys. Rev. B* **1988**, *37*, 785.

(16) Schreckenbach, G.; Hay, P. J.; Martin, R. L. *Inorg. Chem.* **1998**, *37*, 4442.

(17) Schreckenbach, G.; Hay, P. J.; Martin, R. L. *J. Comput. Chem.* **1999**, *20*, 70.

(18) Küchle, W.; Dolg, M.; Stoll, H.; Preuss, H. *J. Chem. Phys*. **1994**, *100*, 7535.

(19) Hariharan, P. C.; Pople, J. A. *Theor. Chim. Acta* **1973**, *28*, 213.

(20) (a) Miertus, S.; Scrocco, E.; Tomasi, J. *Chem. Phys.* **1981**, *55*, 117. (b) Tomasi, J.; Presico, M. *Chem. Rev.* **1994**, *94*, 2027. (c) Barone, V.; Cossi, M.; Mennucci, B.; Tomasi, J. *Chem. Phys.* **1997**, *107*, 3210.

(21) Tsushima, S.; Yang, T. X.; Suzuki, A. *Chem. Phys. Lett.* **2001**, *334*, 365.

(22) Tsushima, S.; Suzuki, A. *J. Mol. Struct. (THEOCHEM)* **2000**, *529*, 21−25.

(23) Spencer, S.; Gagliardi, L.; Handy, N. C.; Ioannou, A. G.; Skylaris, C. K.; Willetts, A.; Simper, A. M. *J. Phys. Chem. A* **1999**, *103*, 1831.

(24) Blaudeau, J. P.; Zygmunt, S. A.; Curtiss, L. A.; Reed, D. T.; Bursten, B. E. *Chem. Phys. Lett.* **1999**, *310*, 347.

(25) Antonio, M. R.; Soderholm, L.; Williams, C. W.; Blaudeau, J. P.; Bursten, B. E. *Radiochim. Acta* **2001**, *89*, 17.

(26) Cosentino, U.; Villa, A.; Pitea, D. *J. Phys. Chem. B* **2000**, *104*, 8001.

(27) Martin, R. L.; Hay, P. J.; Pratt, L. R. *J. Phys. Chem. A* **1998**, *102*, 3565.

(28) Zhang, Y. J.; Collison, D.; Livens, F. R.; Powell, A. K.; Wocadlo, S.; Eccles, H. *Polyhedron* **2000**, *19*, 1757.

(29) Kowall, T.; Foglia, F.; Helm, L.; Merbach, A. E. *Chem. Eur. J.* **1996**, *2*, 285.

(30) Hemmingsen, L.; Amara, P.; Ansoborlo, E.; Field, M. J. *J. Phys. Chem. A* **2000**, *104*, 4095.

(31) Craw, J. S.; Vincent, M. A.; Hillier, I. H.; Wallwork, A. L. *J. Phys. Chem.* **1995**, *99*, 10181.

(32) Besler, B. H.; Merz, K. M.; Kollman, P. A. *J. Comput. Chem.* **1990**, *11*, 431.

(33) Breneman, C. M.; Wiberg, K. B.; *J. Comput. Chem.* **1990**, *11*, 361.

(34) Case, D. A.; Pearlman, D. A.; Caldwell, J. W.; Cheatham, T. E., III; Ross, W. S.; Simmerling, C. L.; Darden, T. A.; Merz, K. M.; Stanton, R. V.; Cheng, A. L.; Vincent, J. J.; Crowley, M.; Tsui, V.; Radmer, R. J.; Duan, Y.; Pitera, J.; Massova, I.; Seibel, G. L.; Singh, U. C.; Weiner, P. K.; Kollman, P. A. *AMBER 6*; University of California, San Francisco. 1999.

(35) Jorgensen, W. L.; Chandrasekhar, J.; Madura, J. D.; Impey, R. M.; Klein, M. L. *J. Chem. Phys.* **1983**, *79*, 926.

(36) Kowall, T.; Foglia, F.; Helm, L.; Merbach, A. E. *J. Am. Chem. Soc.* **1995**, *117*, 3790.

(37) Guardia, E.; Padro, J. A. *J. Phys. Chem.* **1990**, *94*, 6049.

(38) Pearlman, D. A.; Case, D. A.; Caldwell, J. W.; Ross, W. S.; Cheatham, T. E.; Debolt, S.; Ferguson, D.; Seibel, G.; Kollman, P. *Comput. Phys. Commun.* **1995**, *91*, 1.

(39) Gschneidner, K. A.; Eyring, J. L.; Choppin, G. R.; Lander, G. H. *Handbook on the Physics and Chemistry of Rare Earths*, 18 Vol.; Lanthanides/Actinides: Chemistry; North-Holland: Amsterdam, 1994; Chapter 127, p 538.

(40) Impey, R. W.; Madden, P. A.; McDonald, I. R. *J. Phys. Chem.* **1983**, *87*, 5071.

(41) Beveridge, D. L.; Mezei, M.; Mehrotra, P. K.; Marchese, F. T.; Ravishanker, G.; Vasu, T.; Swaminathan, S. *Adv. Chem. Ser.* **1983**, *204*, 297.

(42) Mountain, R. D. *J. Chem. Phys.* **1989**, *90*, 1866.

(43) (a) Durand, S.; Dognon, J. P.; Guilbaud, P.; Rabbe, C.; Wipff, G. *J. Chem. Soc., Perkin Trans.* **2000**, *4*, 705. (b) Baaden, M.; Berny, F.; Madic, C.; Wipff, G. *J. Phys. Chem. A* **2000**, *104*, 7659. (c) Cieplak, P.; Kollman, P.; Lybrand, T. *J. Chem. Phys.* **1990**, *92*, 6755. (d) Cieplak, P.; Caldwell, J.; Kollman, P. *J. Comput. Chem.* **2001**, *22*, 1048. (e) Warshel, A.; King, G. *Chem. Phys. Lett.* **1985**, *121*, 124. (f) Strajbl, M.; Sham, Y. Y.; Villa, J.; Chu, Z. T.; Warshel, A. *J. Phys. Chem. B* **2000**, *104*, 4578.

(44) Sánchez Marcos, E.; Martínez, J. M.; Pappalardo, R. R. *J. Chem. Phys.* **1998**, *108*, 1752.